pH-responsive polymer–drug conjugates as multifunctional micelles for cancer-drug delivery

2014 Nanotechnology 25 335101

(http://iopscience.iop.org/0957-4484/25/33/335101)

IOP Publishing Nanotechnology
Nanotechnology **25** (2014) 335101 (12pp) doi:10.1088/0957-4484/25/33/335101

pH-responsive polymer–drug conjugates as multifunctional micelles for cancer-drug delivery

Yang Kang[1], Wei Ha[1], Ying-Qian Liu[3], Yuan Ma[1], Min-Min Fan[2], Li-Sheng Ding[1], Sheng Zhang[2] and Bang-Jing Li[1]

[1] Key Laboratory of Mountain Ecological Restoration and Bioresource Utilization, Chengdu Institute of Biology, Chinese Academy of Sciences, Chengdu, 610041, People's Republic of China
[2] State Key Laboratory of Polymer Materials Engineering, Polymer Research Institute of Sichuan University, Sichuan University, Chengdu, 610041, People's Republic of China
[3] State School of Pharmacy, Lanzhou University, Lanzhou, 730000, People's Republic of China

E-mail: libj@cib.ac.cn and zslbj@163.com

Received 10 February 2014, revised 25 April 2014
Accepted for publication 30 April 2014
Published 30 July 2014

Abstract

We developed a novel linear pH-sensitive conjugate methoxy poly(ethylene glycol)-4β-aminopodophyllotoxin (mPEG-NPOD-I) by a covalently linked 4β-aminopodophyllotoxin (NPOD) and PEG via imine bond, which was amphiphilic and self-assembled to micelles in an aqueous solution. The mPEG-NPOD-I micelles simultaneously served as an anticancer drug conjugate and as drug carriers. As a drug conjugate, mPEG-NPOD-I showed a significantly faster NPOD release at a mildly acidic pH of 5.0 and 4.0 than a physiological pH of 7.4. Notably, it was confirmed that this drug conjugate could efficiently deliver NPOD to the nuclei of the tumor cells and led to much more cytotoxic effects to A549, Hela, and HepG2 cancer cells than the parent NPOD. The half maximal inhibitory concentration (IC_{50}) of mPEG-NPOD-I was about one order magnitude lower than that of the NPOD. *In vivo*, mPEG-NPOD-I reduced the size of the tumors significantly, and the biodistribution studies indicated that this drug conjugate could selectively accumulate in tumor tissues. As drug carriers, the mPEG-NPOD-I micelles encapsulated hydrophobic PTX with drug-loading efficiencies of 57% and drug-loading content of 16%. The loaded PTX also showed pH-triggered fast release behavior, and good additive cytotoxicity effect was observed for the PEG-NPOD-I/PTX. We are convinced that these multifunctional drug conjugate micelles have tremendous potential for targeted cancer therapy.

S Online supplementary data available from stacks.iop.org/NANO/25/335101/mmedia

Keywords: micelle, anticancer, drug carrier, podophyllotoxin, pH-responsible cleavage

1. Introduction

In recent years, stimuli-sensitive drug delivery systems have emerged as appealing systems in which the release of drugs can be readily modulated by exerting an appropriate stimulus. The stimuli-responsive release of a cytotoxic drug may enhance their therapeutic efficacy and minimize side effects. It is known that the pH around tumors, other hypoxic disease tissues, and intracellular compartments such as endosomes and lysosomes of cells is more acidic (i.e., 5.5 to 6.5) relative to normal physiological pH (i. e., 7.4) [1]. Therefore, this pH variation is considered an ideal trigger for the selective release of anticancer drugs in a tumor or in its vicinity, accomplishing tumor-targeted drug delivery.

pH-responsive nanocarriers (including polymeric particles [2], liposomes [3], and dendrimers [4]) and pH-responsive polymer-drug conjugates (polymeric prodrugs) [5] are two major syste12ms for drug delivery at present. The nanocarriers can load various drugs simply by self-assembly and tend to dissociate and release the loaded drugs in response to the changes in environmental pH values. Furthermore, the nanoscale of the carriers also leads to an

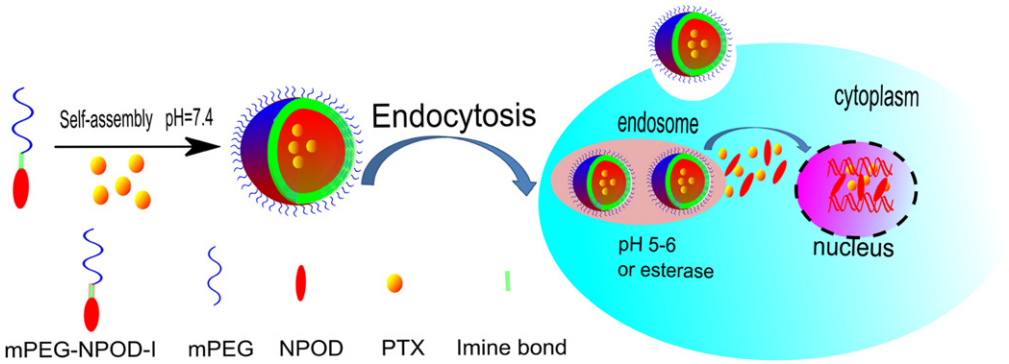

Scheme 1. Illustration of mPEG-NPOD-I conjugates selectively releasing drugs in cancer cells.

accumulation in the cancerous tissues via the tumors' enhanced permeability and retention (EPR) effect [6, 7]. However, these systems have disadvantages, including low loading efficiency, low loading content, and varied loading contents from batch to batch. pH-responsive polymeric prodrugs covalently link the polymer and drugs through acid labile spacers, which have high drug-loading content and can release drugs at a specific site without premature drug release. A certain drawback of polymer-drug conjugates is that they require cost studies to determine safety and efficacy as new drug entities, while they cannot carry various drugs like nanocarriers.

Is there any approach to combine the advantages of nanocarriers and polymer-drug conjugates? Recently, Shen *et al* [8, 9] have developed a kind of amphiphilic drug-polymer conjugate, which not only serves as a prodrug but also forms vesicles or micelles to carry other drugs for combination therapy. Although not possessing specific release mediated pH-sensitivity, this novel approach arouses the interest of many researchers regarding the design of a new multifunctional drug delivery system.

In this study, we developed a pH-sensitive amphiphilic drug-polymer conjugate, which could form stable micelles in aqueous conditions. As a drug-polymer conjugate, this conjugate had a fixed and high drug-loading content. Once in a tumor or in its vicinity, these conjugates released an active drug, enhancing the cytotoxicity *in vitro* and *vivo*. As drug carriers, the micelles could carry other anticancer drugs, such as paclitaxel (PTX), to combine their anticancer efficacies. Hydrophobic 4β-aminopodophyllotoxin (NPOD), a derivative of podophyllotoxin (POD), was selected as a model drug because 1) POD and its derivatives, such as etoposide, teniposide, and etopophos (etoposide phosphate), are anticancer agents with high activity against leukemia, lung, ovary, lymphoma, bladder and other serious cancers [10–12] but have not been well applied due to the side effects caused by nonspecific cytotoxicity; 2) The therapeutic utility of POD and some of its derivatives are hindered by extremely low water solubility (<1 μg ml^{-1}) [13, 14]. Methoxy poly(ethylene glycol) (mPEG) was selected as the hydrophilic component due to its good water solubility and excellent biocompatibility, as well as for the fact that it is non-adhesive to proteins [15–17]. Scheme 1 illustrated the formation of polymer-drug conjugate micelles loaded PTX, and the micelles selectively release drugs at endosomal compartments. Herein, the synthesis of pH-responsive methoxy poly (ethylene glycol)-*block* –4β-aminopodophyllotoxin (mPEG-*b*-NPOD or mPEG-NPOD-I), the formation of mPEG-*b*-NPOD micelles, the pH-dependent drug release, the intracellular release and trafficking of NPOD, *in vitro* drug efficacy, *in vivo* pharmacokinetics and biodistribution of mPEG-*b*-NPOD micelles, and the utility of mPEG-*b*-NPOD micelles as carriers for other drugs were investigated.

2. Experimental section

2.1. Materials and instruments

The materials and instruments used in this paper are described in the supporting information.

2.2. Preparation of the NPOD derivatives

The brief procedures for mPEG-POD and for mPEG-NPOD-A are described in the supporting information, while the procedure for mPEG-NPOD-I is as follows:

mPEG(MW = 750) (4.01 g, 5.45 mmol), p-CBA (0.82 g, 5.46 mmol), and DMAP (0.33 g, 0.27 mmol) were mixed in 30 ml anhydrous dichloromethane; the solution was then cooled to 0 °C. Subsequently, DCC (1.34 g, 6.51 mmol) was added to the solution under a nitrogen atmosphere; the solution was stirred for 24 h at 0 °C. The solution was evaporated in a vacuum, and the residue was purified by silica column chromatography, eluted with DCM/ Acetone (5:1) to remove the residual DCU, and followed with DCM/methanol (5:1) to produce the pure product mPEG-CHO (**3**) as a colorless viscous oil, 4.34 g (90.3%). ^{1}H NMR (600 MHz, $CDCl_3$): δ 9.99 (s, 1 H), 8.19 (d, J = 8.4 Hz, 2 H), 7.93 (d, J = 8.4 Hz, 2 H), 4.46 (t, 2 H), 3.62 (br, 58 H), 3.30 (s, 3 H).

NPOD (0.59 g, 1.43 mmol) was added to a solution of mPEG-CHO (1.05 g, 1.21 mmol) in ethanol (30 ml); the reaction mixture was refluxed overnight, then evaporated in a vacuum and followed by liquid chromatography on Sephadex LH-20 gel with methanol as eluent to give the pure product mPEG-NPOD-I **1** 1.38 g (90.8%, yellow viscous oil). ^{1}H NMR (600 MHz, $CDCl_3$): δ 8.73 (s, 1 H), 8.01 (d, J = 8.4 Hz,

2 H), 7.93 (d, J = 8.4 Hz, 2 H), 6.85 (s, 1 H), 6.53 (s, 1 H), 6.34 (s, 2 H), 5.96 (s, 1 H), 5.90 (s, 1 H), 4.76 (d, J = 3.6 Hz, 1 H), 4.65 (d, J = 5.4 Hz, 1 H), 4.39 (m, 3 H), 4.32 (dd, J = 6, 9.6 Hz, 1 H), 3.80 (dd, J = 15.6, 8.4 Hz, 1 H), 3.57 (s, 6 H), 3.62 (br, 58 H), 3.44 (s, 3 H), 3.41 (s, 3 H), 3.09 (m, 1 H).

2.3. Preparation of the mPEG-NPOD-I micelles and PTX- or Nile Red-loaded mPEG-g-NPOD-I micelles

mPEG-NPOD-I micelles were prepared under stirring conditions and by dropwise adding 10 ml deionized water to 1.0 ml of THF solution that contained 10 mg mPEG-NPOD at room temperature. The resulting solution was stirred overnight to allow complete evaporation of THF. Then, the solution was loaded into a dialysis bag (MWCO 3500) and dialyzed against 5 L of deionized water for 2 days.

To prepare the PTX-loaded micelles, 10 ml deionized water was dropwise added to a mixture of 1.0 ml of mPEG-NPOD solution in THF (10 mg ml^{-1}) and 100 μl paclitaxel solution in DMSO (5 mg ml^{-1}) under stirring at room temperature, followed by ultrasonication for 0.5 h. The mixture solution was then loaded into a dialysis bag (MWCO 3500) and dialyzed against 5 L deionized water for 2 days. The preparation process of Nile red-loaded micelles was similar to the PTX-loaded micelles except the dialysis process was carried out in darkness.

2.4. Micellar characterization

The method to determine the critical micelle concentration (CMC) of mPEG-NPOD-I was the same as that described in our previous work [18]. Pyrene was used as a fluorescence probe. The concentration of the prodrug with the imide bond was varied from 0.0005 to 3 mg ml^{-1}, and the concentration of pyrene was fixed at 1.0 μM. Fluorescent spectra were measured using a fluorescence spectrophotometer with a slit width of 10.0 and 2.5 nm for excitation and emission. For fluorescence emission spectra, excitation wavelength was set at 339 nm, and for fluorescence excitation spectra, the emission wavelength was set at 390 nm.

The CMC of PTX-loaded mPEG-NPOD-I micelles was determined by surface tension methods. The concentration of PTX-loaded mPEG-NPOD-I micelles varied from 0.001 to 1 mg ml^{-1}, and data were obtained using a contact angle meter with the pendant drop method at 25 °C.

The size of the micelles in the aqueous solutions were measured by dynamic light scattering (DLS) at 25 °C using a Coherent innove 304 laser electronic source at the wavelength 532 nm; the scattering angle is 90°. Each sample was measured three times, and the results shown are the mean diameter for two replicate samples.

The morphology of the micelles was observed by a transmission electron microscope (TEM) and scanning electron microscopy (SEM). Samples solution (10 mg ml^{-1}) were dropped onto a copper grid and dried at room temperature. They were examined without being stained. TEM observations were performed at an accelerating voltage of 80 kV and 300 kV. SEM observations were performed on a Jeol JSM-5900LV electron microscope at an accelerating voltage of 20 kV. The samples (micelle concentration of 1 mg ml^{-1}) were prepared by directly dropping the nanoparticle solution onto a slice of silicon and drying the solution at room temperature overnight for SEM studies.

2.5. The pH-dependent hydrolysis rate of the mPEG-NPOD-I

The hydrolysis of mPEG-NPOD-I with imide bond at different pH values (4.0, 5.0, and 7.4) was performed as follows: first, the micelles solution was prepared as 2.4 described. Then, a 2 ml micelles solution was loaded into a dialysis bag (MWCO = 3500) and dialyzed against 10 ml of PBS at 37 °C with constant shaking. 4 ml medium was removed and replaced by 4 mL of fresh PBS to maintain submersed conditions at desired time intervals. The released amount of the NPOD was determined using fluorescence with a slit width of 10.0 and 2.5 nm for excitation and emission. The emission wavelength was 324 nm and the excitation wavelength was 280 nm. The release experiments were carried out in triplicate. The results presented are the average data.

2.6. The drug-loading content and encapsulation efficiency of the micelles

The micelles solution encapsulated the PTX, and the blank micelles solutions were prepared with an equal amount of polymer-drug conjugate at the same conditions at the same time. The PTX content in the solution was determined by its UV-absorption at the wavelength of 230 nm. After the encapsulation process was completed, the UV- absorption of the micelles solution encapsulated the PTX, and the blank micelles solution was detected at the wavelength of 230 nm; then, the absorption of PTX was obtained by subtracting the absorption of the blank micelles solution with the solution encapsulated by the PTX. The standard curves were made using known concentrations of PTX. Drug-loading content and drug encapsulation efficiency were calculated according to the following formula:

$$\text{Drug loading content}(\%) = \frac{W_{\text{drug in nanocapsules}}}{W_{\text{nanocapsules}}} \times 100$$

$$\text{Encapsulation efficiency}(\%) = \frac{W_{\text{drug in nanocapsules}}}{W_{\text{drug used in encapsulation}}} \times 100$$

2.7. The release of paclitaxel from mPEG-NPOD-I micelles

The release profiles of paclitaxel from micelles were carried out under the same conditions of pH-dependent hydrolysis as the mPEG-NPOD-I micelles. And the concentration of the paclitaxel in the PBS buffer solution was determined with the same method to carry out the drug-loading content and encapsulation efficiency.

2.8. In vitro anticancer activities

The biocompatibility of the drug-polymer conjugate was evaluated using the MTT assay in a 96-well plate method.

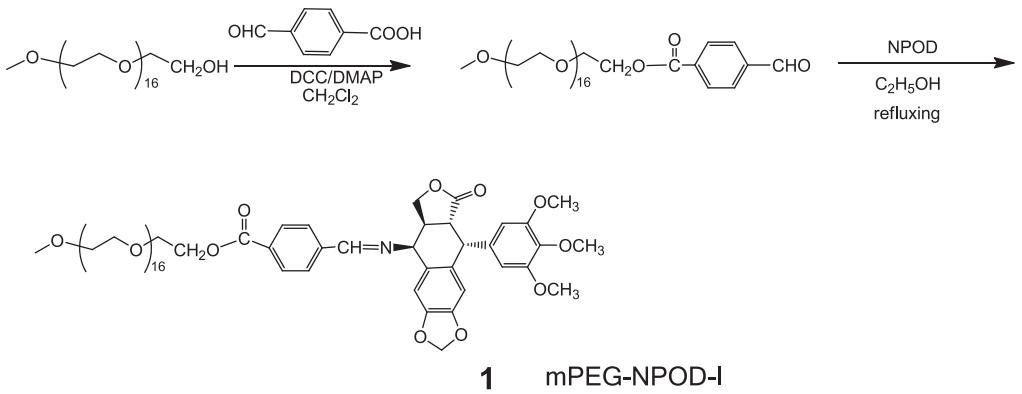

1 mPEG-NPOD-I

Scheme 2. Synthesis of mPEG-NPOD-I.

A549, HepG2, or Hela cells were cultured in 96 well culture plates at a density of 8000 cells per well in a RPMI 1640 medium supplemented with 10% fetal bovine serum at 37 °C in a humidified environment of 5% CO_2 for 1 day. The cells were then incubated with PTX, VP-16, NPOD, PEG-CHO, and drug conjugates at varying concentrations of 0.01–100 μmol by a RPMI 1640 medium containing 10% fetal bovine serum and incubated for another 72 h at 37 °C in a humidified environment of 5% CO_2. Then, the RPMI 1640 medium was aspirated and replaced with 100 μl fresh RPMI 1640 medium containing 10% fetal bovine serum for 24 h. Then, 15 μl 5 mg ml^{-1} MTT solution was added to each well and incubated for an additional 4 h at 37 °C in a humidified environment of 5% CO_2. The medium solution was then replaced with 150 μl DMSO to dissolve the MTT-formazan that was generated by live cells, and the plate were shaken for 30 min to produce a homogeneous colored solution. The absorbance was then read at wavelength 570 nm on a microplate reader. The relative cell viability (%) was determined by comparing the absorbance at wavelength 570 nm with control cells containing only a cell culture medium at wavelength 570 nm. The experiments were carried out six times, and the results presented are the average data.

2.9. Cellular uptake and localization of drug conjugate micelles

About 30 000 A549 cells in 2 mL of RPMI-1640 medium containing 10% fetal bovine serum were seeded per well in 6-well culture plates that contained a sterile glass coverslip in each well. Then, the plate was incubated for 24 h at 37 °C in a humidified environment of 5% CO_2 and 95% air. The original medium was then removed and replaced with 2 mL of fresh medium and dropped into 100 μl of nile red-loaded mPEG -NPOD-I micelles. At the appropriate time point, the RPMI 1640 medium was aspirated, and the cells were rinsed three times with PBS. Then, 0.5 mL of 4% paraformaldehyde was dropped into each well to fix the cells for 15 min. Then, the paraformaldehyde was aspirated; after being rinsed three times with PBS, the cells were stained with 0.5 mL 1 μg ml^{-1} DAPI solution for 15 min. Then, the DAPI staining solution was removed, and the cells were washed by PBS twice before coverslips were mounted on the slides [19]. Images were taken using a Nikon Eclipse Ti-E microscope. Nile red was observed using a Cy3 filter expressed as red, and DAPI was observed using a DAPI filter expressed as blue.

2.10. Pharmacokinetic and biodistribution studies in mice

Chinese Kun Ming mice (25–30 g) were used to investigate the pharmacokinetic and the biodistribution of the polymer-drug conjugate. The methods were carried out as the previous report described [20–22]. The mice were handled under protocols approved by Sichan University Laboratory Animal Center. The 20 mice were divided into two groups with an equal amount of mice in each group. One group was given 0.1 mL mPEG -NPOD-I micelles (NPOD equivalent 10 mg kg^{-1}) in a PBS solution, and the other group was given 0.1 mL NPOD in 20% ethanol of a PBS solution (NPOD equivalent 10 mg kg^{-1}). Each mouse was intravenously administrated. 50 μl blood samples were collected into 1.5 ml centrifuge tubes at the designated times via drawing from the tail vein, and the weight of the blood samples were recorded. Then, 50 μl of 10% (v v^{-1}) Triton X-100, 100 μl of water, and 750 μl of acidified isopropanol (0.75 N HCl) were added. The tubes were vortexed for 5 min to ensure complete mixing, and NPOD was extracted at −20 °C overnight. Then, tubes were warmed to room temperature, and the fluorescence of supernatant was measured after the tubes were centrifuged at 14 000 rmp for 30 min. For biodistribution studies, Chinese Kun Ming mice were implanted with S180 tumor cells in subaxillary; and 1 week after implantation, the tumors along the subaxillary were well established. Then, 20 mice were divided into two random groups. One group was given the mPEG -NPOD-I with a conversional NPOD dose of 10 mg kg^{-1}; the other group was given a single NPOD dose of 10 mg kg^{-1}. The mice were sacrificed 24 h after the administration. The organs/tissues (0.1 g of each) were wet-weighed and homogenized in 0.5 mL of a cell lysis buffer in a glass homogenizer. Then, 10 μl of tissue lysate was mixed with 5 mL 10% (v v^{-1}) Triton X-100. The tubes were vortexed for 5 min, and 75 μl acidified isopropanol (0.75 N HCl) were added. The mixtures were incubated at −20 °C overnight. The fluorescence of the supernatant was measured after the tubes centrifuged at 14 000 rmp for 30 min.

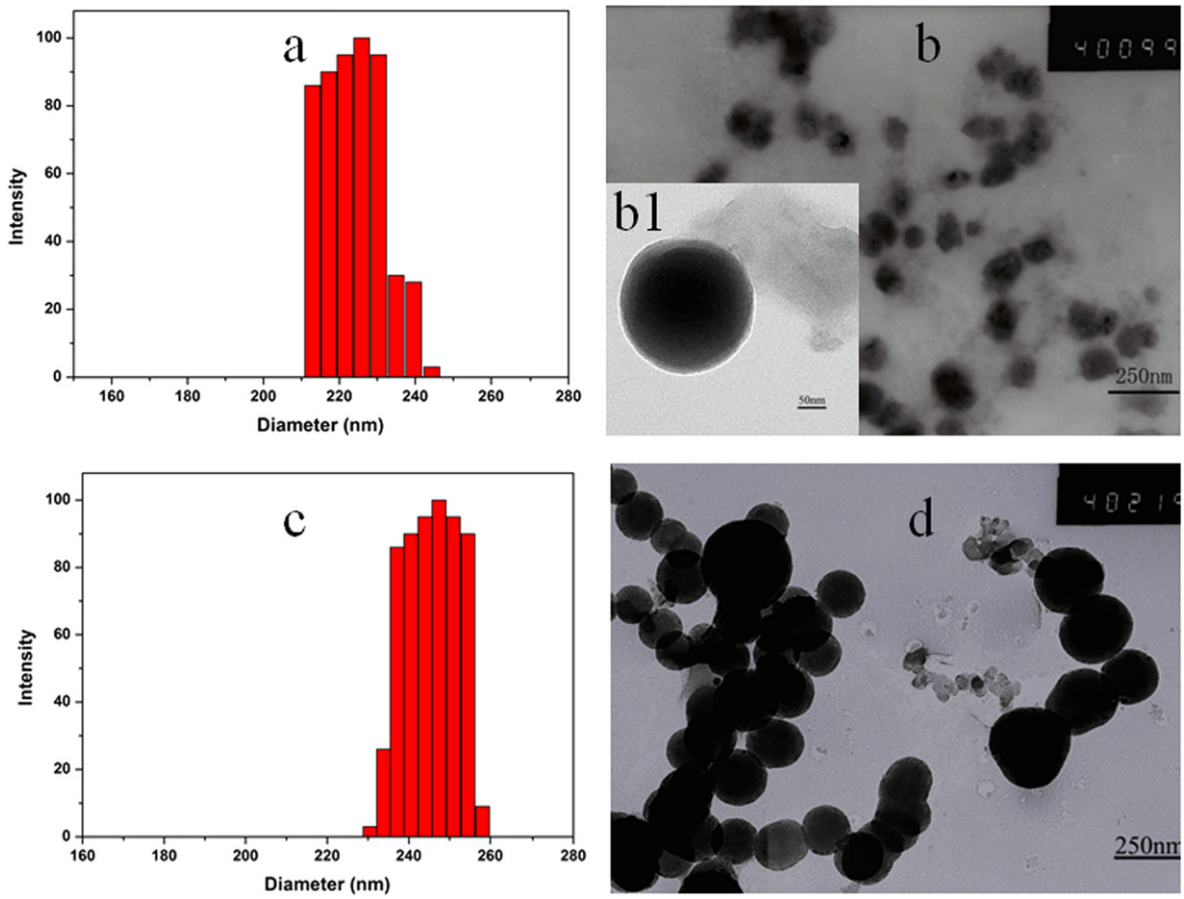

Figure 1. (a) mPEG-NPOD-I-formed micelles measured by dynamic laser light scattering (DLS) and (b) TEM morphology of the micelles (b, scale bar of 250 nm; b1, scale bar of 50 nm). (c) mPEG-NPOD-I-formed micelles measured by dynamic laser light scattering (DLS) after loading with 18.5 wt % hydrophobic PTX and TEM morphology of the micelles after (d, scale bar of 250 nm) loading with 18.5 wt % hydrophobic PTX.

2.11. In vivo anticancer activities

The experiment was carried out using male Chinese Kun Ming mice (25–30 g), and the mice were handled under protocols approved by Sichan University Laboratory Animal Center. 12 mice were divided into two groups with equal amounts and maintained under sterile conditions and at a 12 h light/dark cycle in a temperature-controlled environment. The mice were implanted with S180 tumor cells in subaxillary; and 1 week after implantation, the tumors along the subaxillary were well established. The treatment group (6 mice) was administered with 0.1 mL mPEG -NPOD-I (NPOD equivalent 10 mg kg^{-1}) in a PBS solution per day via the tail vein to each mouse for four consecutive days, and the control group (6 mice) was administered with 0.1 mL PBS solution per day via the tail vein to each mouse for four consecutive days. The mice were monitored and showed no signs of side effects. Then, the mice were sacrificed and all the tumors in their bodies were dissected for the tumor weight per mouse determination after 24 h.

2.12. Maximum tolerated dose (MTD) studies

The normal Kunming mice were divided into 5 groups ($n = 6$) and administered intravenously with saline or mPEG -NPOD-I (10, 20, 30, 40 mg kg^{-1} NPOD equivalents body weight in 200 μL saline) for a single injection and then allowed to recover. Their weight was monitored continuously for 14 days. Changes in body weight and the survival of the mice were measured daily for 15 days. The maximum tolerated dose (MTD) was defined as the maximum dose resulting in less than 15% loss in body weight and not resulting in death [23].

3. Results and discussion

3.1. Synthesis of the mPEG-NPOD-I

It has been reported that PEG could conjugate to PDO through an ester bond or through carbonate. For instance, in a study done by the National Cancer Institute (USA), PEG-PDO ester was screened for activity against 60 different human cancer cell lines, and the desired anticancer properties of PDO were retained [24]. However, the ester bond and carbonate were not sensitive enough to the mildly acidic pH. As far as we know, pH-sensitive PDO-polymer conjugates have not been reported. In this paper, the imide bond was chosen as the pH responsible linking bond for preparation of

polymer-drug conjugates (mPEG-NPOD-I) because it is easy to hydrolyze in a mildly acidic environment. PEG-PDO conjugates can be made water soluble by introducing a long PEG chain ($M_n = 5000$). We proposed that PEG-PDO conjugated with small water-soluble moieties should not be molecularly water soluble, but would be similar to a surfactant-like amphiphilic molecule that self-assembles to micelles in water, leading to high and fixed PDO-loading content. Therefore, an mPEG with an average molecular weight of 750 was selected as the hydrophilic segment of the conjugate, and 4β-aminopodophyllotoxin, a derivative of podophyllotoxin, was selected as the hydrophobic segment of the conjugate. The synthetic procedures of mPEG-NPOD-I are shown in scheme 2. The mPEG with a terminal aldehyde group (mPEG-CHO) was firstly synthesized. Then, the mPEG-NPOD-I with an imine bond as the linkage bond was synthesized by refluxing the mPEG-CHO and NPOD in ethanol for 12 h. The structure of the product was confirmed by ^{1}H NMR The chemical shift at δ 8.73 (s, 1 H) represents the proton of the new formed imide bond. All other chemical shifts of the NMR could be attributed to the corresponding protons of the product; and all the integral ratios of the protons' signals match the theoretical value [25].

In order to compare the pH-sensitivity of mPEG-NPOD-I conjugates with different linkage, mPEG-POD with an ester bond and mPEG-NPOD-A with an amide bond as linkage were also synthesized. (The synthetic procedures and characterization are provided in the supporting information.)

3.2. Formation of the mPEG-NPOD-I micelles

The amphiphilic mPEG-NPOD-I block copolymers in an aqueous solution could form micelles with hydrophobic NPOD cores and hydrophilic mPEG shells. The critical micelle concentration (CMC) of the mPEG-NPOD-I micelles was determined by fluorescence study using pyrene as a probe. As shown in figure S1, at low concentration of mPEG-NPOD-I, pyrene exhibited relatively low fluorescence intensity, indicating that the pyrene was in water and few micelles were present. With the concentration increasing, however, the fluorescence intensity increased remarkably, reflecting the pyrene that was encapsulated in the interior of the micelles. CMC was determined from the crossover point in the low concentration ranges. The CMC of mPEG-NPOD-I micelles is 1.08 mg ml^{-1}.

Dynamic light scattering (DLS) results showed that the mPEG-NPOD-I micelles were about 226 nm with narrow size distributions (PDI = 0.205) (figure 1(a)). Furthermore, the morphology of the micelles was investigated by transmission electron microscopy (TEM) and scanning electron microscopy (SEM). As shown in figure 1(b) and figure S2a, these drug-polymer conjugates were spherical micelles with a size of about 200 nm.

As we discussed, the mPEG-NPOD-I conjugates were amphiphilic and could form nano-sized micelles in an aqueous solution. In the past decades, drug delivery systems based on micelles have attracted considerable attention [26–30] because the hydrophobic core micelles can efficiently load lipophilic therapeutic drugs; meanwhile, the hydrophilic shell can stabilize the aggregates [6, 7]. Compared with conventional amphiphilic copolymers, the hydrophobic drug NPOD replaced the polymer component here.

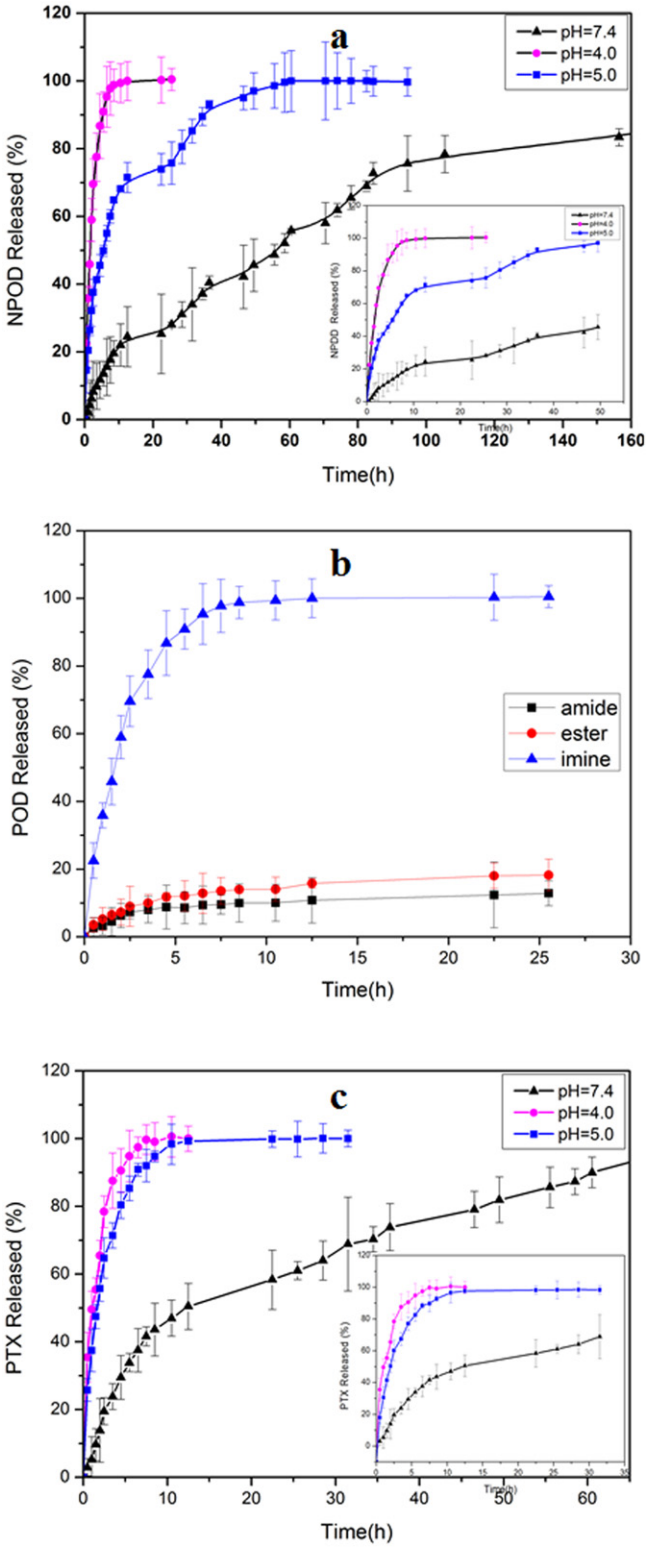

Figure 2. (a), (b) pH-triggered hydrolysis of NPOD in the mPEG-NPOD polymer-drug conjugates and (c) pH-triggered simultaneous release of PTX.

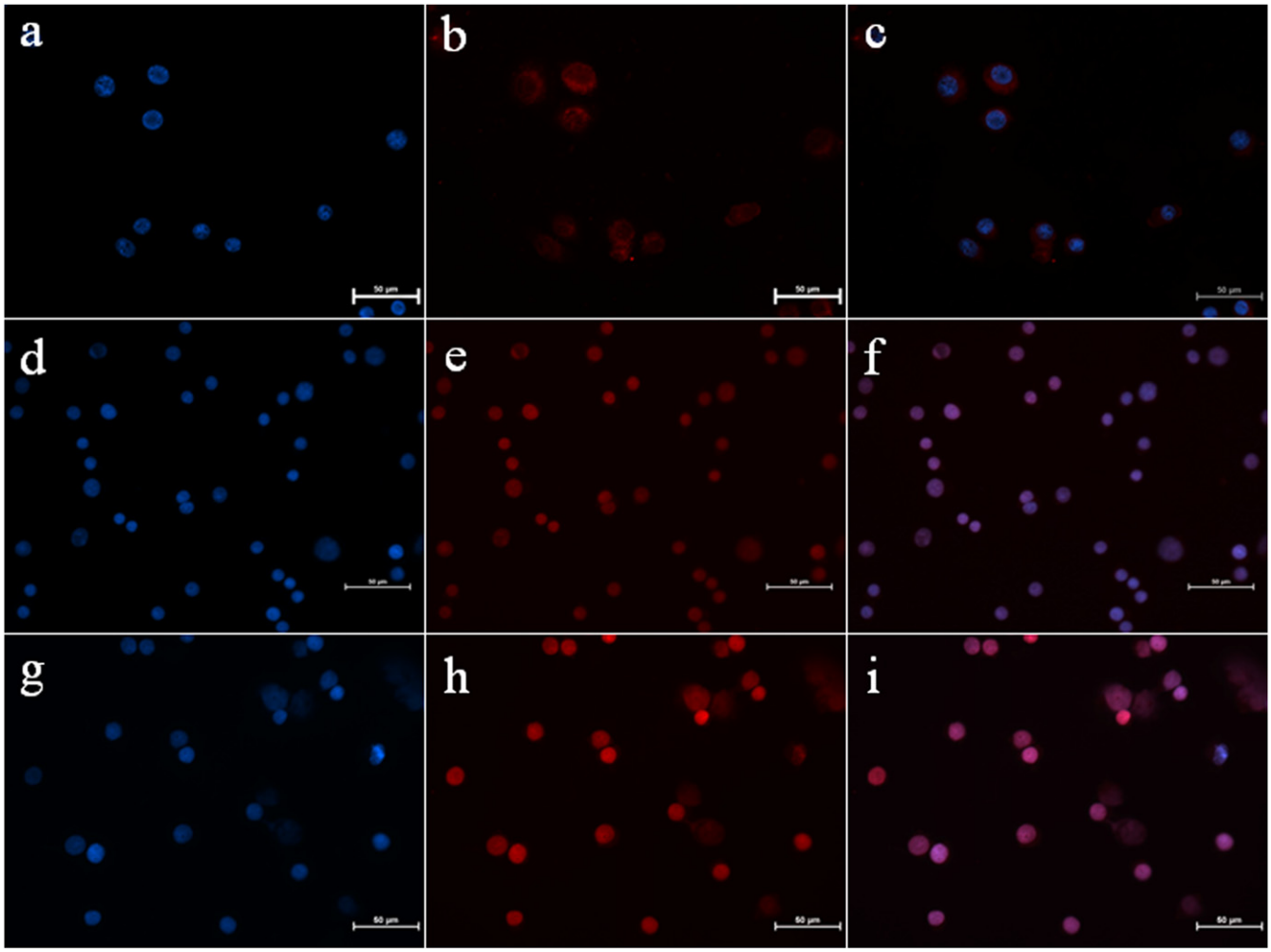

Figure 3. The fluorescent images of A549 lung cancer cells incubated with mPEG-NPOD-I micelles for: (a)–(c) 2, (d)–(f) 12, and (g)–(i) 24 h. For each panel, images from left to right show cell nuclei stained by DAPI (blue), Nile red fluorescence in cells (red), and overlays of two images. The scale bars correspond to 50 μm in all images.

PTX is an anticancer agent effective against a wide range of tumors. It has been reported that the combination of etoposide (a PDO derivative) and paclitaxel demonstrated significant efficacy as a first-line therapy for extensive-stage small cell lung cancer (SCLC) and was well tolerated with no unexpected toxicities [31–33]. Hence, we chose PTX as a model to study loading and pH-triggered release behavior of mPEG-NPOD-I micelles as drug carriers.

PTX was loaded into the micelles using a dialysis method. The loading efficiency was 57%, and the loading content was 16.3 wt %. DLS results showed that the micelles with entrapped PTX were about 247 nm with narrow size distributions (PDI = 0.273) (figure 1(c)), which were a little bigger than the mPEG-NPOD-I micelles without PTX. TEM and SEM revealed homogeneous spherical micelles with a size of about 230 nm (figure 1(d) and figure S2b).

The CMC for the PTX loaded micelles was determined by the surface tension method. Usually, the amphiphilic copolymer concentration is above CMC, and these polymeric micelles are formed to minimize the interfacial energy, while the interfacial tension shows a sudden change at or near CMC; so the surface tension measurements should be carried out over a wide range of concentrations. Figure S3 shows that the surface intension decreases linearly with the logarithmic copolymer concentrations at low concentrations but is flat in the crossover region. So, the CMC of PTX-loaded mPEG-NPOD-I formed micelles determined from the intersection point of those two straight lines was about 0.035 mg ml^{-1}, which was only about 1/30 of that for the mPEG-NPOD-I formed micelles. We hypothesize that this interesting phenomenon should be attributed to the π-π interaction between the NPOD and PTX in the inner core of the formed micelles, which enhanced the hydrophobic property of the mPEG-NPOD-I molecules.

The zeta potential of both the mPEG-NPOD-I-formed micelles and the PTX-loaded mPEG-NPOD-I-formed micelles were 0.23 mV, indicating that the surfaces of both micelles were covered by neutral mPEG.

3.3. In vitro stability and drug release

The NPOD release from mPEG-NPOD-I was investigated under three different pHs (4.0, 5.0, and 7.4) at 37 °C, and the release behavior of NPOD via three different linkages such as

imine bond, ester bond, and the amide bond connect to the mPEG chain at pH 4.0 were also studied. The cumulative release amount of the NPOD was determined by fluorescence spectroscopy method. Interestingly, the results showed that approximately 100 and 70% of NPOD were released in 20 h, at pH 4.0 and 5.0, respectively, from mPEG-NPOD-I. In contrast, only 25% of NPOD was released after 20 h at pH 7.4 (figure 2(a)). These results indicate that mPEG-NPOD-I are acid-sensitive and more likely cleavable at an acidic endosoma or tumor, while stable at a physiological environment. In comparison with mPEG-NPOD-I, an amide bonded conjugate and ester bonded conjugate only showed less than 20% of free NPOD released (figure 2(b)), suggesting that the imine bond is more sensitive than an ester bond and an amide bond. Hence, mPEG-NPOD-I have obvious advantages over other reported PEG-POD conjugates (bonded by ester or amide [27]), that is, enhanced pH-sensitivity and potential for superior site-specific delivery.

The release behaviors of PTX from mPEG-NPOD-I micelles were also investigated at 37 °C in three different pH solutions (4.0, 5.0, and 7.4). As shown in figure 2(c), there was a significantly faster release of PTX from mPEG-NPOD-I micelles at a mildly acidic environment compared to the physiological pH. After 15 h, almost 100% PTX was released at pH = 4.0 and 5.0, whereas only 50% PTX was released at pH = 7.4. Obviously, the lower pH value led to faster release of the drugs. This trend of release behavior had a good consistency with the NPOD release from mPEG-NPOD-I conjugates, indicating that fast drug PTX release at mildly acidic conditions was caused by the hydrolysis of imide linkage.

3.4. Intracellular uptake of the mPEG-NPOD-I

A549 lung cancer cell lines were used for the examination of intracellular drug release behavior of the polymer-drug conjugates. 4β-aminopodophyllotoxin (NPOD), a topoisomerase-II inhibitor, is known to exert drug effects at an endonuclear level and inhibit macromolecular biosynthesis [25]. However, the fluorescence intensity of NPOD is so weak that it could not be observed by a fluorescence microscope; nile red was used as a probe to indicate the locations of micelles when encapsulated into the micelles [34–37]. As shown in figure 3, significant nile red fluorescence was observed around the nuclei of A549 lung cancer cells after 6 h of incubation with nile red entrapped mPEG-NPOD-I micelles. Following 12 h of incubation, more nile red was accumulated at the nuclei of the A549 lung cancer cells, suggesting that more and more micelles were internalized. After 24 h of incubation, nile red was noticeably accumulated at the nuclei of the A549 lung cancer cells. It is interesting that the free nile red stained the membrane and nucleus of the cells simultaneously (Figure S4), but the loaded nile red mainly stained the nucleus of cells. These results indicate that the Nile red-loaded mPEG-NPOD-I-formed micelles are successfully internalized by A549 cells and mainly resided in the nucleus.

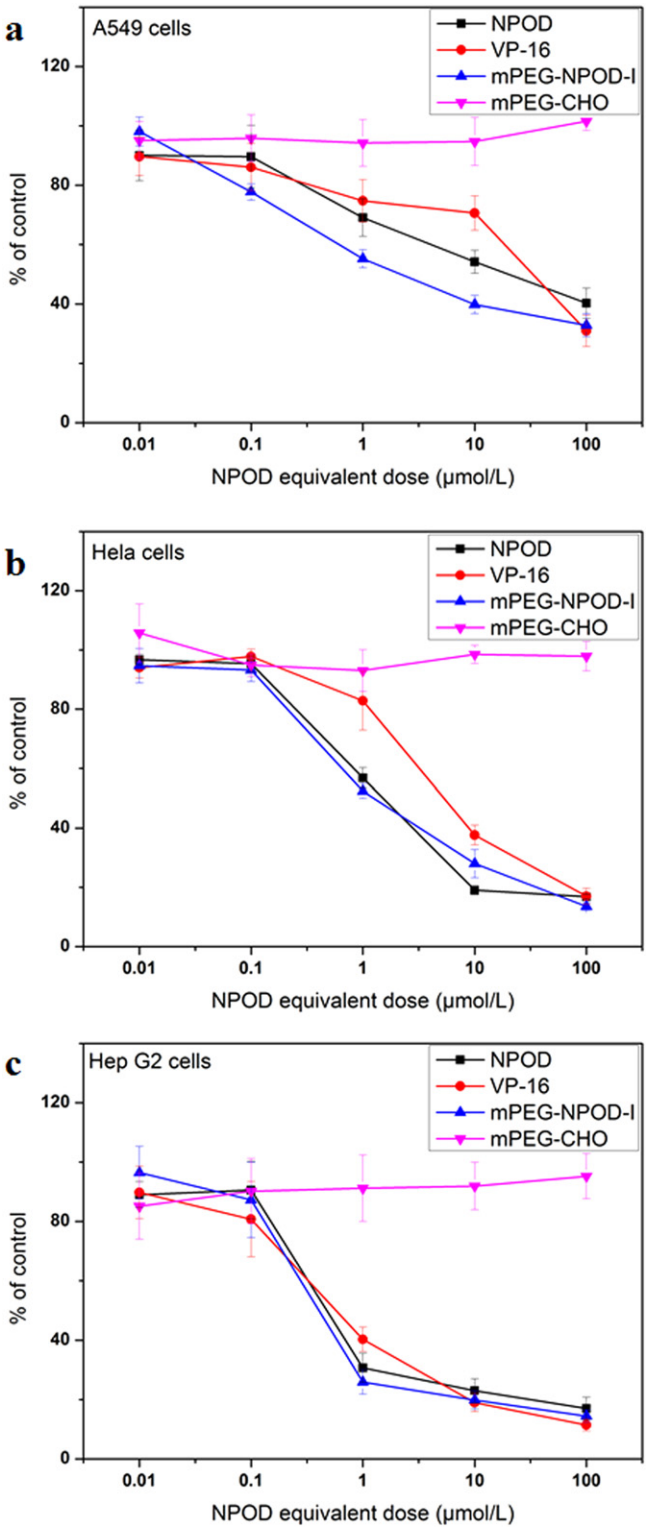

Figure 4. *In vitro* cytotoxicity of NPOD, VP-16, mPEG-NPOD-I and mPEG-CHO to A549 lung cancer cells, Hela cervical cancer cells, and Hep G2 liver cancer cells ((a)–(c) respectively).

3.5. In vitro anticancer activities

The cytotoxicities of mPEG-POD-I, NPOD and mPEG-CHO were investigated in A549, Hela, and Hep G2 cancer cell lines by MTT assays. The results revealed that mPEG-CHO used for synthesizing mPEG-POD-I was nontoxic to all three types

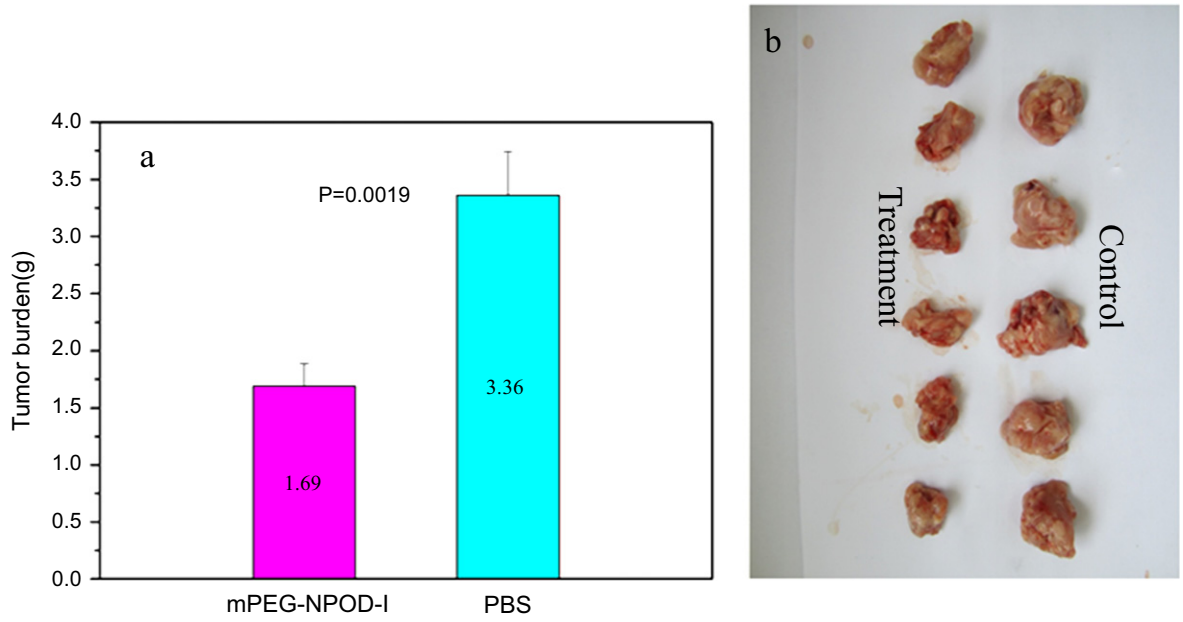

Figure 5. (a) *In vivo* antitumor activity of mPEG-NPOD-I to allografted S180 sarcoma tumors in KM mice. (b) Tumor photographs at the end of the experiment taken from treatment and control groups.

of cells when the tested concentration was up to 100 μmol L^{-1}, indicating that mPEG-CHO inherited the excellent biocompatibility property of PEG. However, under the same conditions, the mPEG-NPOD-I polymer-drug conjugate and NPOD showed pronounced cytotoxicity (figures 4(a)–(c)) to all the investigated cell lines, indicating that mPEG-NPOD-I and NPOD have a broad spectrum of anticancer activity. The activity of mPEG-NPOD-I was much higher than that of NPOD. For example, significantly reduced cell viabilities of about 45.8, 47.6, and 74.1% were observed at a mPEG-NPOD-I at a concentration of 1 μmol NPOD equiv/L for A549, Hela, and HepG2 cancer cells, respectively, while the parent NPOD only reduced cell viabilities of about 30.9, 43.2, and 69.3% at the same concentration. The half maximal inhibitory concentration (IC_{50}) of mPEG-NPOD-I was 3.4 μmol L^{-1} for A549 cancer cells, while IC_{50} of NPOD was 30.2 μmol L^{-1}, which was about one order magnitude higher than that of mPEG-NPOD-I. Therefore, the mPEG-NPOD-I clearly enhanced the cytotoxicity of NPOD. Meanwhile, the mPEG-NPOD-I was found to have high cytotoxicity at a concentration of 1 μmol NPOD equiv/L to all three cancer cell lines in comparison with etoposide (VP-16), a widely-used and important antineoplastic agent that shows good clinical effects against several types of tumors, including testicular and small cell lung cancers, lymphoma, leukemia, and Kaposi's sarcoma [38]. So, all the results obtained above indicate the mPEG-NPOD-I would be a good candidate for cancer treatment.

3.6. In vivo anticancer activities

The therapeutic efficacy of mPEG-NPOD-I was evaluated using KM mice bearing S180 sarcoma tumors in subaxillary. It should be noted that NPOD must be dissolved in a certain proportion of ethanol solution for i.v. administration due to the inherent water insolubility. Use of a large amount of solvent for four consecutive days induced significant allergic reactions and resulted in the death of mice. So the control group (6 mice) was administered with 0.1 ml PBS, not the free NPOD drug. Comparing the treatment group with the control group, mPEG-NPOD-I conjugate showed about 2-fold tumor growth inhibition in the tumor model, confirming the high therapeutic potential (figure 5(a)). Furthermore, no significant weight loss or acute toxicity of mPEG-NPOD-I was observed during the entire period of the experiments. Figure 5(b) showed that mPEG-POD-I reduced the size of the tumors significantly. The significance of the experimental data was determined by a student's t-test ($P < 0.05$), and data are plotted as means ± standard errors (SE).

3.7. Pharmacokinetics and biodistribution studies

Fluorescence spectroscopy was used to determine the NPOD level in the plasma as previous reports described [39, 40]. 50 μl blood samples were collected at the designated times via drawing from the tail vein following a single i.v. injection of mPEG-NPOD-I conjugate (NPOD equivalent 10 mg kg^{-1}) or NPOD formulation (NPOD 10 mg kg^{-1}) in Chinese Kun Ming mice. It should be noted that due to the water insolubility, intravenous administration of free NPOD is difficult except when using organic solvents. As shown in figure 6(a), the peak plasma concentration of the mPEG-NPOD-I treated group was about 45 μg ml^{-1}, which increased by about 29% over that of the NPOD treated group. At all times, NPOD plasma concentrations were higher in the mPEG-NPOD-I treated group than in the NPOD treated group. Moreover, it should be noticed that the use of solvent in the free NPOD formulation might induce hypersensitivity reactions [41],

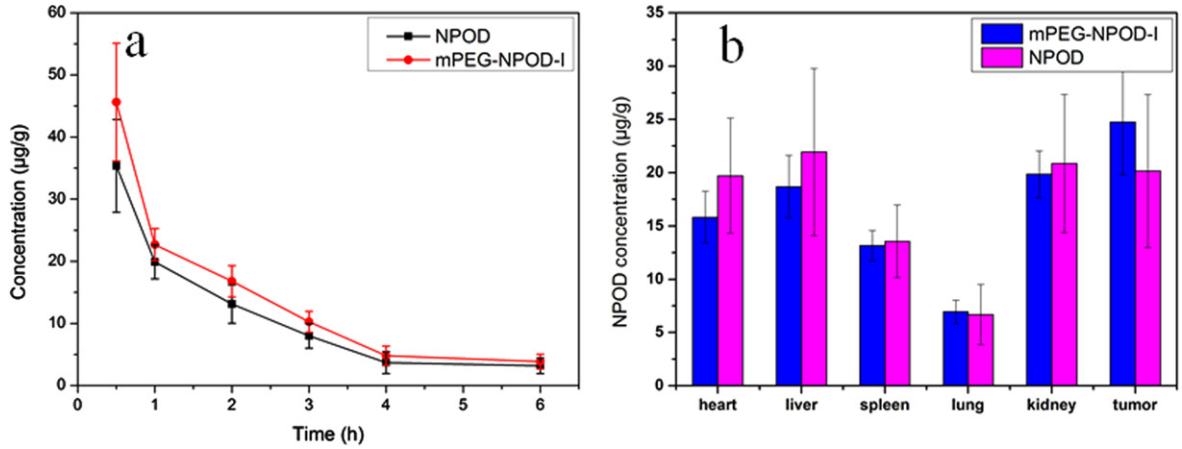

Figure 6. (a) *In vivo* pharmacokinetics and (b) biodistribution of mPEG-NPOD-I prodrug and free NPOD in KM mice ($n = 10$). NPOD uptake is expressed as injected dose per gram of tissue.

while no solubilizing adjuvants were needed for mPEG-NPOD-I conjugates.

The biodistribution of NPOD was determined at 24 h after injection of mPEG-NPOD-I conjugates (NPOD equivalent 10 mg kg^{-1}) in Chinese Kun Ming mice bearing S180 mouse sarcoma. As shown in figure 6(b), the tumor uptake of NPOD for mPEG-NPOD-I conjugates was 25 $\mu g\ g^{-1}$, which increased by 22% over that for free NPOD formulation. This improved bioavailability in a tumor may be attributed to the enhanced permeability and retention (EPR) effect that has been described for other macromolecular drugs [42–44] and the PEG influence. It has been reported that PEG accumulated at the tumor tissue to a higher extent than at the normal tissue, and such high tumor accumulation of PEG showed dependence on the molecular weight of PEG [45]. In the case of mPEG-NPOD-I, the molecular weight of PEG was 750; therefore, the bioavailability in the tumor was indeed improved but not significantly.

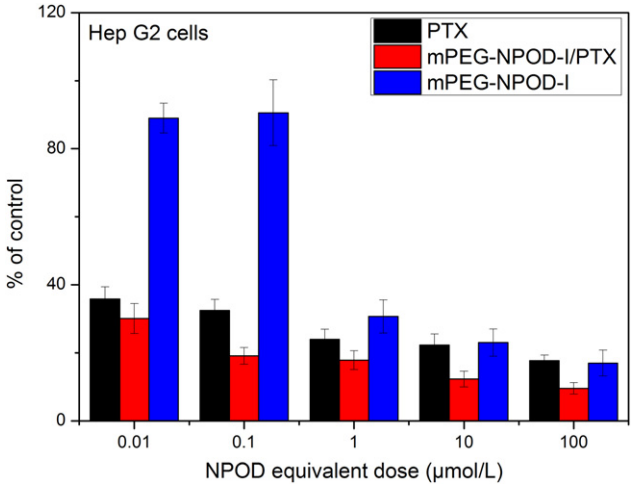

Figure 7. *In vitro* cytotoxicity of PTX, mPEG-NPOD-I and mPEG-NPOD-I/PTX to Hep G2 liver cancer cells.

3.8. Additive effects between mPEG-NPOD-I and loaded PTX

The cytotoxicity of PTX-loaded mPEG-NPOD-I micelles (mPEG-NPOD-I/PTX) against Hep G2 cells were estimated by MTT assay. As shown in figure 7, mPEG-NPOD-I/PTX showed a higher cytotoxicity than mPEG-NPOD-I and free PTX in all the doses tested in the Hep G2 cells. This finding proved the above results showing that mPEG-NPOD-I micelles served as a carrier to deliver PTX into the cells, producing additive anticancer effects. For example, the PTX (0.1 $\mu mol\ L^{-1}$) alone killed about 67.5% of the cells, while the mPEG-POD-I loaded 0.1 $\mu mol\ L^{-1}$ PTX killed approximately 82.2% cells. The cytotoxicity of mPEG-NPOD-I/PTX increased 21.7%.

3.9. Maximum tolerated dose studies

It should be noted that free PTX must be dissolved in a certain proportion of ethanol or other organic solution for i.v. administration due to the inherent water insolubility. However, use of a large amount of solvent for i.v. administration induced significant allergic reactions and resulted in the death of mice. As shown in figure 8, there was only 4% body weight loss and no toxic death for the mice treated with mPEG-NPOD-I-formed micelles at a NPOD equivalent dosage as high as 20 mg kg^{-1}; even when mice were treated with mPEG-NPOD-I-formed micelles at a NPOD equivalent dosage as high as 30 mg kg^{-1}, only about 6% body weight loss and one death occurred. From the present study, it can be estimated that the single i.v. MTD for mPEG-NPOD-I-formed micelles with equivalent doses of NPOD was at least 20 mg kg^{-1} to 30 mg kg^{-1}, which was almost equal with that of Taxol® in the previous report [46]. The high MTD for mPEG-NPOD-I-formed micelles may be attributed to the controlled release kinetics of NPOD almost without burst release under physiological conditions and to the remarkable biocompatibility and safety of the PEG.

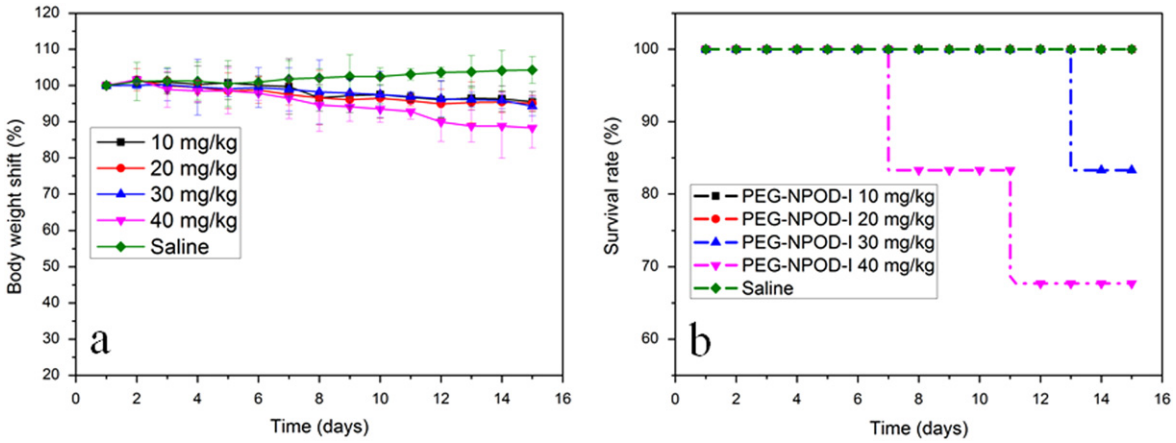

Figure 8. MTD studies for mPEG-NPOD-I-formed micelles on (a) body weight change and (b) survival rate in tumor-free Kunming mice.

4. Conclusion

In summary, we have successfully prepared a kind of linear pH-sensitive polymer-drug conjugate by directly conjugating the insoluble NPOD to the end of PEG via an acid labile imine bond with a fixed and high drug-loading content of NPOD by as much as 36 wt%. This conjugate showed a significantly faster NPDO release at a mildly acidic pH of 5.0 and 4.0 than a physiological pH of 7.4. It is confirmed that the mPEG-NPOD-I conjugate could efficiently deliver NPDO to the nuclear of the tumor cells and led to much more cytotoxic effects to A549, Hela, and HepG2 cancer cells than the parent NPDO. *In vivo*, the mPEG-NPOD-I reduced the size of the tumors significantly, and the biodistribution studies indicated that this conjugate can selectively accumulate in tumor tissues. The MTD results showed the micelles had an excellent safety profile, with a MTD of at least 20 mg kg^{-1} to 30 mg kg^{-1} equivalent dose of NPOD. In addition, because the mPEG-NPOD-I could self-assemble into micelles, it can also act as a carrier to encapsulate hydrophobic PTX with the drug-loading efficiencies of 57.04% and drug-loading content of 16.26%. The loaded PTX also showed that pH-triggered fast release behavior. The mPEG-NPOD-I/PTX delivered two anticancer drugs, producing a good additive cytotoxicity effect at low concentrations to cancer cells. The *in vivo* studies of mPEG-NPOD-I/PTX, including the *in vivo* toxicity, pharmacokinetics, biodistribution, and antitumor activity, will be carried out in our future research. It is believed that these multifunctional polymer-drug conjugate micelles will have potential as intelligent nanovehicles for targeted cancer therapy.

Acknowledgments

This work was funded by the National Natural Science Foundation of China (Grant No. 51373174), the West Light Foundation of CAS, and the CAS Knowledge Innovation Program (Grant No. KSCX2-EW-J-22).

References

[1] Gao Y H, Ma R J, An Y L and Shi L Q 2011 *J. Control. Release* **152** E81–2
[2] Paramonov S E, Bachelder E M, Beaudette T T, Standley S M, Lee C C, Dashe J and Frechet J M J 2008 *Bioconjugate Chem* **19** 911–9
[3] Obata Y, Tajima S and Takeoka S 2010 *J. Control Release.* **142** 267–76
[4] Criscione J M, Le B L, Stern E, Brennan M, Rahner C, Papademetris X and Fahmy T M 2009 *Biomaterials* **30** 3946–55
[5] Aryal S, Hu C M J and Zhang L F 2010 *Acs Nano* **4** 251–8
[6] Wang Z F, Hu X L, Yue J and Jing X B 2011 *J. Control Release* **152** E41–2
[7] Huang P, Lin J, Yang D P, Zhang C L, Li Z M and Cui D X 2011 *J. Control Release* **152** E33–4
[8] Shen Y Q *et al* 2010 *J. Am. Chem. Soc.* **132** 4259–65
[9] Zhou L, Cheng R, Tao H Q, Ma S B, Guo W W, Meng F H, Liu H Y, Liu Z and Zhong Z Y 2011 *Biomacromolecules* **12** 1460–7
[10] Walker G N 1953 *J. Am. Chem. Soc.* **75** 3393–7
[11] Bohlin L and Rosen B 1996 *Drug Discov. Today* **1** 343–51
[12] Hu X M, Gao C M, Tan C Y, Zhang C L, Zhang H L, Li S F, Liu H X and Jiang Y Y 2011 *Protein Peptide Lett.* **18** 1258–64
[13] Xue M, Zhu R R, Qin L L, Li F J, Liu Z X, Sun X Y and Wang S L 2009 *Sci. China Ser.* B **52** 1253–7
[14] Fan L, Wu H, Zhang H, Li F and Yang T H 2010 *Polym. Compos.* **31** 51–9
[15] Khandare J and Minko T 2006 *Prog. Polym. Sci.* **31** 359–97
[16] Aronov O, Horowitz A T, Gabizon A and Gibson D 2003 *Bioconjugate Chem.* **14** 563–74
[17] Greenwald R B, Choe Y H, McGuire J and Conover C D 2003 *Adv. Drug Deliver Rev.* **55** 217–50
[18] Ha W, Wu H, Wang X L, Peng S L, Ding L S, Zhang S and Li B J 2011 *Carbohyd Polym.* **86** 513-9
[19] Tang H D, Murphy C J, Zhang B, Shen Y Q, Van Kirk E A, Murdoch W J and Radosz M 2010 *Biomaterials* **31** 7139–49
[20] Chen H B, Chang X L, Du D R, Liu W, Liu J, Weng T, Yang Y J, Xu H B and Yang X L 2006 *J. Control. Release* **110** 296–306
[21] Qin L L, Xue M, Wang W R, Zhu R R, Wang S L, Sun J, Zhang R and Sun X Y 2010 *Int. J. Pharm.* **388** 223–30
[22] Laginha K M, Verwoert S, Charrois G J R and Allen T M 2005 *Clin. Cancer Res.* **11** 6944–9
[23] Han H and Mark E D 2013 *Mol. Pharmaceutics* **10** 2558–67

[24] Niemczyk H J and Van Arnum S D 2008 *Green Chem. Lett. Rev.* **1** 165–71
[25] Lee K H, Imakura Y, Haruna M, Beers S A, Thurston L S, Dai H J, Chen C H, Liu S Y and Cheng Y C 1989 *J. Nat. Prod.* **52** 606–13
[26] Kabanov A V, Batrakova E V, Miller D and Alakhov V 1997 *Abstr. Pap. Am. Chem. S* **214** 157
[27] Xiong X B, Falamarzian A, Garg S M and Lavasanifar A 2011 *J. Control. Release* **155** 248–61
[28] Dworak C, Schachner M and Gruber H 2011 *Int. J. Artif. Organs* **34** 646
[29] Adams M L, Lavasanifar A and Kwon G S 2005 *J. Pharm. Sci.* **94** 1160
[30] Rosler A, Vandermeulen G W M and Klok H A 2001 *Adv. Drug Deliver Rev.* **53** 95–108
[31] Hartmann J T *et al* 2007 *J. Clin. Oncol.* **25** 5742–7
[32] Reck M, Jagos U, Grunwald F, Kaukel E, Koschel G, von Pawel J, Hessler S and Gatzemeier U 2003 *Lung Cancer-J. Iaslc.* **39** 63–9
[33] Perez E A, Geoffroy F J, Hillman S, Johnson E A, Farr G H, Tazelarr H D, Hatfield A K, Krook J E, Maillard J A, Levitt R and Marks R S 2004 *Lung Cancer-J. Iaslc.* **44** 347–53
[34] Xiao H H, Zhou D F, Liu S, Zheng Y H, Huang Y B and Jing X B 2012 *Acta Biomater.* **8** 1859–68
[35] Benaglia M, Alberti A, Spisni E, Papi A, Treossi E and Palermo V 2011 *J. Mater. Chem.* **21** 2555–62
[36] Vinchon-Petit S, Jarnet D, Paillard A, Benoit J P, Garcion E and Menei P 2010 *J. Neuro-Oncol.* **97** 195–205
[37] Liu J Y, Pang Y, Huang W, Zhu X Y, Zhou Y F and Yan D Y 2010 *Biomaterials* **31** 1334–41
[38] Odwyer P J, Leylandjones B, Alonso M T, Marsoni S and Wittes R E 1985 *New Engl. J. Med.* **312** 692–700
[39] Manouilov K K, McGuire T R, Gordon B G and Gwilt P R 1998 *J. Chromatogr.* B **707** 342–6
[40] Strife R J, Jardine I and Colvin M 1981 *J Chromatogr.* **224** 168–74
[41] Hartmann J T and Lipp H P 2006 *Drug Safety* **29** 209–30
[42] Maeda H 2001 *Adv. Enzyme Regul.* **41** 189–207
[43] Maeda H, Bharate G Y and Daruwalla J 2009 *Eur. J. Pharm. Biopharm.* **71** 409–19
[44] Fang J, Nakamura H and Maeda H 2011 *Adv. Drug Deliver Rev.* **63** 136–51
[45] Murakami Y, Tabata Y and Ikada Y 1997 *Drug Deliv.* **4** 23–31
[46] Wang C, Wang Y J, Wang Y J, Fan M, Luo and Qian Z Y 2011 *Int. J. Pharm.* **414** 251–9